DALTON
FULL PAPER

Kinetics and mechanism of the oxidation of $Mn(II)_{aq}$ by bromate and peroxomonosulfate in the presence of molybdate to form $[Mn^{IV}Mo_9O_{32}]^{6-}$

Annette L. Nolan, Robert C. Burns* and Geoffery A. Lawrance

School of Environmental and Life Sciences, Chemistry Building, The University of Newcastle, Callaghan, New South Wales 2308, Australia. E-mail: csrb@paracelsus.newcastle.edu.au

Received 10th May 2002, Accepted 17th May 2002
First published as an Advance Article on the web 11th July 2002

The oxidation of Mn(II) by both BrO_3^- and HSO_5^- in the presence of MoO_4^{2-}, in weakly acidic solution over the pH ranges 3.9–5.5 and 4.4–5.5, respectively, results in the formation of the heteropolyoxomolybdate $[MnMo_9O_{32}]^{6-}$ in each case. The kinetics of oxidation were studied at 40.0 °C for BrO_3^- and 30.0 °C for HSO_5^-, along with temperature dependence studies, and for each oxidant were found to exhibit solution autocatalytic behaviour. For BrO_3^- the oxidation kinetics followed the expanded rate expression

$$+d[MnMo_9O_{32}^{6-}]/dt = k_{AC(1)}[Mn^{2+}][MnMo_9O_{32}^{6-}][HMoO_4^-]^2[BrO_3^-]$$

based on an examination of the individual $[BrO_3^-]$, pH and actual $[MoO_4^{2-}]$ dependences, with a value for $k_{AC(1)}$ of $9.09(34) \times 10^6$ dm^{12} mol^{-4} s^{-1}. For HSO_5^- the oxidation kinetics followed the expanded two-term rate expression

$$+d[MnMo_9O_{32}^{6-}]/dt = k_{AC(2a)}[Mn^{2+}][MnMo_9O_{32}^{6-}][HMoO_4^-]^{-5}[SO_5^-] + k_{AC(2b)}[Mn^{2+}][MnMo_9O_{32}^{6-}][HMoO_4^-]^{-5}[HSO_5^-]$$

based on $[HSO_5^-]$, pH and $[MoO_4^{2-}]$ dependences. The values of $k_{AC(2a)}$ and $k_{AC(2b)}$ are $4.6(4) \times 10^{-11}$ dm^{-9} mol^3 s^{-1} and $2.6(4) \times 10^{-15}$ dm^{-9} mol^3 s^{-1}. For BrO_3^- oxidation, from the composition of the transition state, it is proposed that the product $[MnMo_9O_{32}]^{6-}$ species combines with Mn(II) and two $HMoO_4^-$ ions to generate a Mn(II)-substituted lacunary $[Mn^{II}Mn^{IV}Mo_{11}O_{39}]^{6-}$ anion based on a Keggin structure, with the Mn(IV) located at the centre of the polyoxomolybdate framework. Extended-Hückel molecular orbital calculations have been used to investigate the stability of the proposed Mn(II)-substituted lacunary species, based on an α-Keggin structure, relative to the unassembled components. For HSO_5^- oxidation, the two parallel pathways indicate oxidation by both HSO_5^- and its deprotonated form SO_5^-. The two mechanisms reflect the differences in how BrO_3^- and HSO_5^- operate oxidatively and have been highlighted by the facile nature of polyoxomolybdate polymerization. In each case following oxidation of Mn(II) to Mn(IV) fast separation of the two Mn(IV) centres must subsequently occur, along with rapid assembly of the polyoxomolybdate frameworks around each centre to yield the product species.

Over the past few years we have been involved in a program of investigation of the kinetics of formation of heteropolyoxometalates, from which mechanistic information regarding their assembly can be obtained. Such systems have received little attention in the past, which is associated with the complexity of the structures themselves, and the difficulties in establishing the actual speciation of isopolyoxometalate species (Mo and W) in solution under acid conditions. We have used the strategy involving oxidation of a heteroatom in a low oxidation state in the presence of excess MoO_4^{2-} or WO_4^{2-}, thereby generating the central heteroatom in a higher oxidation state surrounded by a polyoxometalate framework. To date, the kinetics of formation of $[Mn^{IV}Mo_9O_{32}]^{6-}$ from oxidation of Mn(II) by hypochlorous acid (HOCl) and peroxomonosulfate (HSO_5^-), of $[Ni^{IV}Mo_9O_{32}]^{6-}$ from oxidation of Ni(II) by peroxodisulfate ($S_2O_8^{2-}$), and of $[H_4Co^{III}{}_2Mo_{10}O_{38}]^{6-}$ from oxidation of Co(II) by HSO_5^-, all in aqueous solution in the presence of added molybdate, have been studied.[1–4] We have also examined the oxidation of $[Co^{II}W_{12}O_{40}]^{6-}$ to $[Co^{III}W_{12}O_{40}]^{5-}$ using HSO_5^- under both strong (0.05–0.625 M) and weak (pH 4.2–5.7) acid conditions, with the former exhibiting zero-order kinetics while maintaining an intact polyoxotungstate framework, while the latter was found to involve polyoxotungstate fragmentation, oxidation of Co(II) and reassembly of the polyoxotungstate framework.[5]

The oxidation of Mn(II) in aqueous solution has been the subject of numerous studies, where solid manganese dioxide is usually reported as the major product.[6] Manganese dioxide is highly insoluble and its formation plays an important role in the reaction kinetics. The solid formed catalyses further reaction in a classic heterogeneous autocatalytic mechanism. In other instances MnO_4^- can be found as a product in addition to MnO_2, as in oxidation by iodate.[7] However, in the presence of other oxoanions such as molybdate and tungstate under weakly acidic conditions, the soluble manganese(IV) heteropolyoxometalates $[MnMo_9O_{32}]^{6-}$ and $[MnW_6O_{24}]^{8-}$ are obtained rather than MnO_2 and there is no evidence for the formation of higher manganese oxidation states.[1,2,8]

In the study of the kinetics of oxidation of Mn(II) in the presence of molybdate using HOCl to give $[MnMo_9O_{32}]^{6-}$, the observed rate law contained first order concentration terms for MoO_4^{2-} and $HMoO_4^-$, while in the study of the kinetics of oxidation of Co(II) in the presence of molybdate using HSO_5^- to give (principally) $[H_4Co_2Mo_{10}O_{38}]^{6-}$, it was shown that two partially built heteropolyoxomolybdate cages can fuse together to produce the dimeric heteropolyoxomolybdate species, $[H_4Co_2Mo_{10}O_{38}]^{6-}$, again involving monomeric $HMoO_4^-$ units rather than preformed polymeric species such as $[Mo_7O_{24}]^{6-}$.[1,4] From these studies it was concluded that the major building blocks as regards polyoxomolybdate assembly are $HMoO_4^-$

DOI: 10.1039/b204832a

and MoO_4^{2-}. The polymeric polyoxomolybdate anions simply act as reservoirs of the monomeric species, which are in fast equilibria with the polymeric species. Similarly, electrospray ionisation mass spectrometry (ESI-MS) of both isopolyoxomolybdates and -tungstates has shown that $HMoO_4^-$ and HWO_4^- are again the likely sources of the polymerization units in the assembly of polyoxo-molybdate and -tungstate frameworks under non-equilibrium conditions.[9,10]

In the present study we report the formation of $[MnMo_9O_{32}]^{6-}$ using BrO_3^- as the oxidant under weakly acidic conditions, which provides further insight into the assembly of polyoxomolybdate cages. In addition, oxidation by HSO_5^- has been re-examined in the light of our latter studies and comparisons with the previously examined oxidant, HOCl, are also made.

The studies show that in all cases $[MnMo_9O_{32}]^{6-}$ forms by an autocatalytic mechanism, with the product $[MnMo_9O_{32}]^{6-}$ species playing an active role in the formation of the transition state as part of the oxidation process. The studies also provide evidence for the mechanism of assembly of polyoxometalate frameworks, and for molybdate in particular, involving the formation of transition states that can be related to well-known heteropolyoxometalates that exhibit the Keggin, *e.g.* $[X^{n+}M_{12}O_{40}]^{(8-n)-}$ [X = P(V), As(V), Si(IV), Ge(IV); M = Mo or W] and Anderson, *e.g.* $[Y^{n+}Mo_6O_{24}H_6]^{(6-n)-}$ [Y = Cr(III), Co(III), Ni(II), Zn(II)] structures. The differences in the transition states appear to be related to the coordination of the oxidant and likely depend on the electron transfer requirements of the oxidant during the oxidation process, with BrO_3^- and HSO_5^- requiring monodentate and bidentate coordination, respectively.

Experimental

Kinetic studies

Reactions were performed on a Hitachi 150-20 spectrophotometer fitted with a thermostatted compartment stable to ±0.1 °C, with all reactions monitored at 480 nm. Millipore Milli-Q water was used throughout the kinetic studies. Equal volumes of buffered solutions containing Mn^{2+}/MoO_4^{2-} and BrO_3^- or HSO_5^- were mixed to obtain the final solutions. All pH measurements were made with a Hanna Instruments 8521 pH meter, coupled to a HI 1131B glass electrode. Final reaction mixtures contained variable amounts of $MnSO_4 \cdot H_2O$ (UNIVAR, AR Grade), $Na_2MoO_4 \cdot 2H_2O$ (UNIVAR, AR Grade) and either $NaBrO_3$ (Aldrich, 99.9+%) or $2KHSO_5 \cdot KHSO_4 \cdot K_2SO_4$ ("Oxone", Aldrich, purity 97.4%, obtained titrimetrically) as appropriate, with enough $NaNO_3$ (UNIVAR, AR Grade) to yield a total ionic strength of 1.00 M. For the molybdate dependence studies, however, in order to obtain a wide range of Mn^{2+} : MoO_4^{2-} ratios, solutions were prepared with a total ionic strength of 1.50 M. All reaction mixtures were initially prepared using 5 M acetic acid/NaOH buffer solutions. The high concentration of buffer solutions was necessary to stabilise the pH due to the basicity of MoO_4^{2-} in solution during polymerisation to generate (primarily) $[Mo_7O_{24}]^{6-}$. As a result, only very slight variations in pH were observed over the range of MoO_4^{2-} concentrations used at any fixed pH and, similarly, minor variations in pH were observed over the range of oxidant concentrations used. Discussion of the analysis of the data is given below.

Extended-Hückel molecular orbital studies

Extended-Hückel molecular orbital calculations were performed using the package described by Mealli and Proserpio[11] (Version 4.0, 1994), with the extended-Hückel parameters, *i.e.* Coulomb integrals, H_{ii} (eV) and Slater exponents (ζ), taken from the values provided in the package. The Wolfsberg–Helmholtz constant was set to 1.75. For $[MnMo_9O_{32}]^{6-}$, the X-ray crystallographic coordinates were taken from the reported structure of $K_6[MnMo_9O_{32}] \cdot 6H_2O$,[2] while for the α-Keggin geometry of the hypothetical $[Mn^{IV}Mn^{II}Mo_{11}O_{39}]^{6-}$ ion, the coordinates were derived from that of α-$[GeMo_{12}O_{40}]^{4-}$ in $Na_4[GeMo_{12}O_{40}] \cdot 8H_2O$[12] with Mn(IV) replacing Ge(IV) because of their identical crystal radii,[13] and the Mn(II) replacing a peripheral Mo(VI) (along with its terminal O^{2-} ligand). For $[Mn(OH_2)_6]^{2+}$, all Mn–O distances were set to 2.160 Å,[14] with O–H distances of 0.97 Å and an H–O–H angle of 104.5°. The geometry for $HMoO_4^-$ was based on a tetrahedrally coordinated Mo(VI), with all Mo–O distances of 1.75 Å and an O–H distance of 0.97 Å, and a Mo–O–H angle of 109.5°. The water molecule had O–H distances of 0.97 Å, with an H–O–H angle of 104.5°.

Table 1 Observed rate constants for oxidation of Mn(II) by BrO_3^- in the presence of MoO_4^{2-}: oxidant dependence ($[Mn^{2+}]$ = 0.0025 M, $[MoO_4^{2-}]_T$ = 0.0625 M, pH = 5.03 ± 0.02, I = 1.00 M, 40.0 °C)

$[BrO_3^-]$/M	$k_{ac(1)}$/dm^3 mol^{-1} s^{-1}	$10^5[MnMo_9O_{32}^{6-}]_i$/M
0.10	0.14(1)	1.4
0.20	0.27(1)	1.9
0.30	0.40(2)	1.4
0.40	0.54(3)	1.1
0.50	0.65(4)	1.3

Results and discussion

A. Oxidation of Mn(II) by BrO_3^- in the presence MoO_4^{2-}

Oxidation of Mn(II) by BrO_3^- in the presence MoO_4^{2-} over the pH range 3.94–5.52 occurred very slowly at room temperature (>24 h for oxidant concentrations from 0.1–0.5 M). The pH range is narrow because of the limitation imposed by the range of stability reported for the product species.[15] All oxidation kinetics were subsequently monitored at 40.0 (±0.1) °C, with the exception of the temperature dependence study. Based on the known molar absorptivity of $[MnMo_9O_{32}]^{6-}$ at 480 nm,[2] complete conversion to this species occurred under the range of experimental conditions employed in the present study. Examination of a range of $[BrO_3^-]/[Mn^{2+}]$ values, with $[Mn^{2+}]$ = 0.0025 M, $[MoO_4^{2-}]$ = 0.0625 M and pH = 5.10 at 40.0 °C, indicated that the stoichiometry was 0.40 mole of BrO_3^- per mole of Mn^{2+}. The overall reaction can therefore be written as in eqn. (1).

$$5Mn^{2+} + 45MoO_4^{2-} + 52H^+ + 2BrO_3^- \longrightarrow 5[MnMo_9O_{32}]^{6-} + 26H_2O + Br_2 \quad (1)$$

The absorbance–time traces for the formation of $[MnMo_9O_{32}]^{6-}$ exhibited typical "S-shaped" curves, which are characteristic of autocatalysis, and which have been previously observed for the oxidation of Mn(II) in the presence of MoO_4^{2-} using the oxidant HOCl.[1] Consequently, the kinetic data were analysed in terms of a second order autocatalytic reaction that obeys rate law (2), where $k_{ac(1)}$ is a pseudo-second order rate constant which subsumes dependences on $[BrO_3^-]$ and, as will be shown below, second order dependences on both $[MoO_4^{2-}]$ and $[H^+]$.

$$+d[MnMo_9O_{32}^{6-}]/dt = k_{ac(1)}[Mn^{2+}][MnMo_9O_{32}^{6-}] \quad (2)$$

The rate constants were obtained using the standard treatment for second order autocatalysis.[16] Thus a plot of $\ln[(A_t/A_\infty)/(1 - A_t/A_\infty)]$ against time gives a straight line of slope $k_{ac(1)}[Mn^{2+}]_i$, where $[Mn^{2+}]_i$ is the initial concentration of Mn(II) and, from the intercept (y) on the ordinate axis, a measure of the "initial" product concentration, $[MnMo_9O_{32}^{6-}]_i$, which is "instantly" formed on mixing the two solutions containing the starting reagents ($[MnMo_9O_{32}^{6-}]_i = [Mn^{2+}]_i e^y$). The rate constants are listed in Tables 1–4 along with the $[MnMo_9O_{32}^{6-}]_i$ values obtained under the various conditions.

Table 2 Observed rate constants for oxidation of Mn(II) by BrO_3^- in the presence of MoO_4^{2-}: pH dependence ($[Mn^{2+}] = 0.0025$ M, $[BrO_3^-] = 0.40$ M, $[MoO_4^{2-}]_T = 0.0625$ M, $I = 1.00$ M, 40.0 °C)

pH	$10^2[MoO_4^{2-}]_{calc}$/M	$k_{ac(1)}$/dm^3 mol^{-1} s^{-1}	$10^5[MnMo_9O_{32}^{6-}]_i$/M
3.94	0.0405	0.30(2)	6.5
4.37	0.126	0.40(2)	4.8
4.57	0.214	0.47(3)	3.3
4.82	0.411	0.51(3)	2.2
5.03	0.709	0.54(3)	1.1
5.34	1.56	0.58(3)	3.4
5.52	2.44	0.59(3)	6.8

Dependences on BrO_3^-, H^+ and MoO_4^{2-}. The autocatalytic rate constant showed a first order dependence on $[BrO_3^-]$ at pH 5.03. The data are given in Table 1. A plot of log $k_{ac(1)}$ against log $[BrO_3^-]$ generated a linear relationship, with a slope of 1.00(2) ($R^2 = 0.9993$), giving the expanded rate expression (3), where $k'_{ac(1)}$ is 1.34(2) dm^6 mol^{-2} s^{-1} at 40.0 °C.

$$+d[MnMo_9O_{32}^{6-}]/dt = k'_{ac(1)}[Mn^{2+}][MnMo_9O_{32}^{6-}][BrO_3^-] \quad (3)$$

Notably, no deviation from first order behaviour was observed, as BrO_3^- is not protonated under the pH conditions used in the present study. Further discussion of possible protonation of BrO_3^- is given below, following the establishment of the H^+ dependence.

In order to determine the potential dependences of the rate on $[H^+]$ and $[MoO_4^{2-}]$, the variations of $k_{ac(1)}$ with pH and with total added molybdate, *i.e.* $[MoO_4^{2-}]_T$, were examined. The data are listed in Tables 2 and 3, respectively. The variation with pH appears to be complex, as shown in Fig. 1, while at a pH of 5.29,

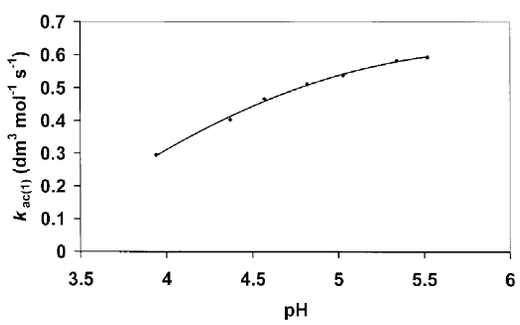

Fig. 1 Dependence of $k_{ac(1)}$ on pH. $[Mn^{2+}] = 0.0025$ M, $[BrO_3^-] = 0.040$ M, $[MoO_4^{2-}]_T = 0.0625$ M, $I = 1.00$ M, 40.0 °C.

$k_{ac(1)}$ shows a non-linear relationship with $[MoO_4^{2-}]_T$, as shown in Fig. 2(a). This behaviour is a result of changes in the speciation of molybdate with both pH and concentration, primarily from the polymerization reaction given by $7MoO_4^{2-} + 8H^+ \longrightarrow Mo_7O_{24}^{6-} + 4H_2O$. There have been a number of studies on the speciation of molybdate with both pH and concentration.[17–19] The present study was carried out at $I = 1.00$ M for the pH dependence and $I = 1.50$ M for the molybdate dependence in acetic acid–NaOH buffer solutions. While no speciation studies have been carried out in this medium, previous studies have shown that the formation constants

Table 4 Observed rate constants for oxidation of Mn(II) by BrO_3^- in the presence of MoO_4^{2-}: temperature dependence ($[Mn^{2+}] = 0.0025$ M, $[BrO_3^-] = 0.50$ M, $[MoO_4^{2-}]_T = 0.0625$ M, pH = 5.11, $I = 1.00$ M)

Temperature/°C	$k_{ac(1)}$/dm^3 mol^{-1} s^{-1}	$10^6[MnMo_9O_{32}^{6-}]_i$/M
25.7	0.26(1)	0.8
30.0	0.41(2)	5.5
34.9	0.55(2)	2.7
40.0	0.67(3)	10.5
45.0	0.84(4)	24.7

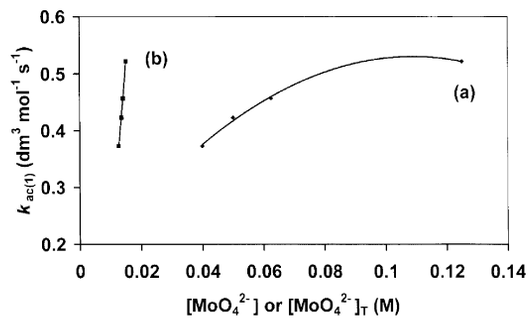

Fig. 2 Dependence of $k_{ac(1)}$ on (a) total added molybdate, $[MoO_4^{2-}]_T$ and (b) actual $[MoO_4^{2-}]$ in solution. $[Mn^{2+}] = 0.0025$ M, $[BrO_3^-] = 0.040$ M, pH = 5.29, $I = 1.50$ M, 40.0 °C.

reported by Ozeki *et al.*[17,18] in 3 M $NaClO_4$ are satisfactory for the purposes of calculating the actual MoO_4^{2-} concentration in solution in an acetic acid–NaOH buffer.

Using the molybdate speciation to determine the actual MoO_4^{2-} concentration in solution, *i.e.* $[MoO_4^{2-}]_{calc}$, for various amounts of total added molybdate, at constant pH, the actual MoO_4^{2-} dependence may be investigated. The actual variation of $k_{ac(1)}$ with $[MoO_4^{2-}]_{calc}$ is shown in Fig. 2(b). From this data, a plot of log $k_{ac(1)}$ against log $[MoO_4^{2-}]_{calc}$ gave a linear relationship with a slope of 1.93(3) ($R^2 = 0.9994$), which indicates a second order dependence on $[MoO_4^{2-}]_{calc}$. The second order dependence on $[MoO_4^{2-}]_{calc}$ can now be included in the rate expression to give the expanded rate expression (4), where $k''_{ac(1)}$ is 2.82(4) × 10^4 dm^{12} mol^{-4} s^{-1} at 40.0 °C based on the actual MoO_4^{2-} concentration present in solution at a pH of 5.03 as calculated from the reported formation constants.

With the dependence of $k_{ac(1)}$ on $[MoO_4^{2-}]$ now established, it is possible to investigate the actual dependence of $k_{ac(1)}$ on $[H^+]$

$$+d[MnMo_9O_{32}^{6-}]/dt = k''_{ac(1)}[Mn^{2+}][MnMo_9O_{32}^{6-}][MoO_4^{2-}]^2[BrO_3^-] \quad (4)$$

by removing the molybdate dependence at each pH value. A plot of log $\{k_{ac(1)}/[MoO_4^{2-}]^2\}$, using the appropriate $[MoO_4^{2-}]_{calc}$ values, against log $[H^+]$ generated a linear relationship of slope of 2.07(2) ($R^2 = 0.9997$) indicating a second order dependence on $[H^+]$. Thus the rate expression may be further expanded to include this dependence, as in eqn. (5), where $k'''_{ac(1)}$ is 3.20(12) × 10^{14} dm^{18} mol^{-6} s^{-1} at 40.0 °C.

$$+d[MnMo_9O_{32}^{6-}]/dt = k'''_{ac(1)}[Mn^{2+}][MnMo_9O_{32}^{6-}][H^+]^2[MoO_4^{2-}]^2[BrO_3^-] \quad (5)$$

Table 3 Observed rate constants for oxidation of Mn(II) by BrO_3^- in the presence of MoO_4^{2-}: molybdate dependence ($[Mn^{2+}] = 0.0025$ M, $[BrO_3^-] = 0.40$ M, pH = 5.29 ± 0.01, $I = 1.50$ M, 40.0 °C)

Total $[MoO_4^{2-}]$/M	$10^2[MoO_4^{2-}]_{calc}$/M	$k_{ac(1)}$/dm^3 mol^{-1} s^{-1}	$10^5[MnMo_9O_{32}^{6-}]_i$/M
0.040	1.27	0.37(2)	7.4
0.050	1.36	0.42(2)	7.2
0.0625	1.41	0.46(3)	5.9
0.125	1.51	0.52(3)	1.2

The value for $k'''_{ac(1)}$ is an average over each of the pH values (3.94–5.52) examined in the present study.

At this point it is possible to write eqn. (5) in two alternative forms, by combining the $[H^+]^2$ dependence with either the $[MoO_4^{2-}]^2$ dependence or the $[BrO_3^-]$ dependence. The latter is commonly found in the form $(a + b[H^+]^2)[BrO_3^-]$, where a and b are experimentally determined rate constants, and has been observed in the oxidation of $[Fe(bipy)(CN)_4]^{2-}$, $[Fe(bipy)_2(CN)_2]$ and $[Fe(bipy)_3]^{2+}$ (where bipy = 2,2′-bipyridyl), $IrCl_6^{3-}$, $[Fe(CN)_6]^{4-}$ and $[Co^{II}W_{12}O_{40}]^{6-}$.[20–23] This has been interpreted in terms of two parallel pathways involving oxidation by BrO_3^- and $H_2BrO_3^+$, respectively, with the latter reacting directly with the substrate in the rate-determining step or undergoing a dissociation into H_2O and BrO_2^+ prior to the rate-determining step. It should be stressed that the $[H^+]^2$ dependence has been found only under highly acidic conditions, that is with $[H^+]$ = 0.05–1.50 M.[20–23] No terms in just $[H^+]$ were observed in the above studies, although more complex dependences have been observed, again under acid conditions.[24] Given the pH range employed in the present studies, therefore, it is unlikely that the observed $[H^+]^2$ dependence is associated with the BrO_3^- ion. Moreover, over the pH range actually used in this work, $HMoO_4^-$ is the major monomeric Mo(VI)-containing species in solution, along with MoO_4^{2-}.[17,18] Thus, an alternative form of this rate expression would involve a combination of the dependences on both $[H^+]$ and $[MoO_4^{2-}]$ through the protonation equilibrium $H^+ + MoO_4^{2-} \rightleftharpoons HMoO_4^-$, for which log β = 3.773.[18] This, in turn, leads to rate expression (6), where $k_{AC(1)} = 9.09(34) \times 10^6$ dm^{12} mol^{-4} s^{-1} at 40.0 °C.

$$+d[MnMo_9O_{32}^{6-}]/dt = k_{AC(1)}[Mn^{2+}][MnMo_9O_{32}^{6-}][HMoO_4^-]^2[BrO_3^-] \quad (6)$$

The expression is not unrealistic and simply involves the Mn(II) substrate, the product, *i.e.* $[MnMo_9O_{32}]^{6-}$, as is required for an autocatalytic process, along with the simple monomeric molybdate species, $HMoO_4^-$, as well as the oxidant, BrO_3^-.

Temperature dependence. The temperature dependence of the reaction was studied from 25.7–45.0 °C, and the data are given in Table 4. An Arrhenius plot of ln $k_{ac(1)}$ against $1/T$ produced a non-linear relationship. If it is assumed that the Arrhenius activation energy, E_a, remains constant with temperature for this system, then the non-linear nature of the plot suggests that there is some change in the actual $[MoO_4^{2-}]$ in solution, resulting from a change in polymerization (*i.e.* speciation) over the temperature range studied. In our previous study on the formation of $[MnMo_9O_{32}]^{6-}$ through oxidation of Mn(II) by HOCl in the presence of molybdate,[1] a change in polymerization with temperature was proposed as the cause of the variation in the slope of the Arrhenius plot with temperature. In that study, the temperature range examined was 4.8–20.0 °C. Not surprisingly, therefore, changes in polymerization appear to occur at lower temperatures (the HOCl study) and to higher temperatures (the present BrO_3^- study) relative to the data obtained at room temperature, for which the formation constants apply. It appears that the formation constants reported by Ozeki *et al.*[17,18] are satisfactory for the determination of the actual $[MoO_4^{2-}]$ in solution over the temperature range of about 5 to 40 °C in an acetic acid–NaOH buffer. However, the slight variations from the ideal orders of both the molybdate and H^+ dependences that were observed above may have their origin in slight variations in polymerization at the temperatures employed in the present study. The value of E_a varied from about 76 to 39 kJ mol^{-1} (limiting values), decreasing as the temperature decreased over the range studied. The average value was 46 kJ mol^{-1} (R^2 = 0.969). The temperature dependence data were also used to estimate the enthalpy and entropy of activation for the present reaction (using autocatalytic rate constants from which the dependences on $[MoO_4^{2-}]$, $[H^+]$ and $[BrO_3^-]$ had been removed), and gave $\Delta H^‡$ = 43 kJ mol^{-1} and $\Delta S^‡$ = 170 J K^{-1} mol^{-1}. Solvation effects can be expected to dominate in reactions between ionic species, so that the large positive activation entropy for the reaction indicates significant solvent rearrangement during formation of the transition state. This is consistent with a significant decrease in solvation of the individual components on assembly of the transition state. However, in view of the complexity of the reaction mechanism, as suggested by the rate law, the calculated activation energy really represents a composite value taken over all of the steps contributing to the reactions leading to the transition state.

Mechanistic considerations. The rate law determined above can be used to propose a possible reaction mechanism for the formation of $[MnMo_9O_{32}]^{6-}$. The mechanism for the oxidation of Mn(II) by BrO_3^- in the presence of MoO_4^{2-} can be expressed by steps (7)–(14).

$$5Mn^{II} + 5HMoO_4^- \underset{k_{-1}}{\overset{k_1}{\rightleftharpoons}} 5[Mn^{II}HMoO_4]^+ \quad (7)$$

$$5[Mn^{II}HMoO_4]^+ + 5HMoO_4^- \underset{k_{-2}}{\overset{k_2}{\rightleftharpoons}} 5[Mn^{II}(HMoO_4)_2] \quad (8)$$

$$5[Mn^{II}(HMoO_4)_2] + 5[Mn^{IV}Mo_9O_{32}]^{6-} \underset{k_{-3}}{\overset{k_3}{\rightleftharpoons}} 5[Mn^{IV}Mn^{II}(H_2O)Mo_{11}O_{39}]^{6-} \quad (9)$$

$$[Mn^{IV}Mn^{II}(H_2O)Mo_{11}O_{39}]^{6-} + BrO_3^- \xrightarrow{k_4} [Mn^{IV}Mn^{III}(H_2O)Mo_{11}O_{39}]^{5-} + BrO_3^{2-} \quad (10)$$

$$[Mn^{IV}Mn^{III}(H_2O)Mo_{11}O_{39}]^{5-} + BrO_3^- \longrightarrow [Mn^{IV}Mn^{IV}(H_2O)Mo_{11}O_{39}]^{4-} + BrO_3^{2-} \quad (11)$$

$$2BrO_3^{2-} + 4H^+ \rightleftharpoons 2BrO_2 + 2H_2O \quad (12)$$

$$4[Mn^{IV}Mn^{II}(H_2O)Mo_{11}O_{39}]^{6-} + 2BrO_2 + 8H^+ \longrightarrow 4[Mn^{IV}Mn^{IV}(H_2O)Mo_{11}O_{39}]^{4-} + Br_2 + 4H_2O \quad (13)$$

$$5[Mn^{IV}Mn^{IV}(H_2O)Mo_{11}O_{39}]^{4-} + 35MoO_4^{2-} + 30H^+ \longrightarrow 10[Mn^{IV}Mo_9O_{32}]^{6-} + 20H_2O \quad (14)$$

The third step, (9), involving the competing rates k_3 and k_{-3}, is required to create the observed autocatalysis. The rate-determining step, (10), is followed by the fast reactions (11) to (14), with the final step involving rapid breakdown of the fully oxidized double Mn(IV)-containing species, which involves attack from $HMoO_4^-$ and/or MoO_4^{2-} ions to generate the $[Mn^{IV}Mo_9O_{32}]^{6-}$ product species by fast polyoxomolybdate framework assembly around each separated Mn(IV) ion. The equations involving BrO_3^- are similar to those used for the oxidation of, for example, $[Co^{II}W_{12}O_{40}]^{6-}$, $[Fe(bipy)_3]^{2+}$ and $IrCl_6^{3-}$,[3,21–23] while the sum of the proposed steps (7)–(14) in the above mechanism correspond to the stoichiometry that was described above [eqn. (1)].

Now, from the fast pre-equilibria (7)–(9), which occur prior to the actual oxidation step, expression (15) can be derived.

$$[Mn^{IV}Mn^{II}(H_2O)Mo_{11}O_{39}]^{6-} = \frac{k_1k_2k_3}{k_{-1}k_{-2}k_{-3}}[Mn^{2+}][Mn^{IV}Mo_9O_{32}^{6-}][HMoO_4^-]^2 \quad (15)$$

As the kinetic equation for the rate-determining step is (16), combining eqns. (15) and (16) yields expression (17) for the rate-determining step, which may be written as (18) where $k_{AC(1)} = k_1k_2k_3k_4/k_{-1}k_{-2}k_{-3}$. This is equivalent to the experimentally determined kinetic eqn. (6), assuming that the pre-equilibria

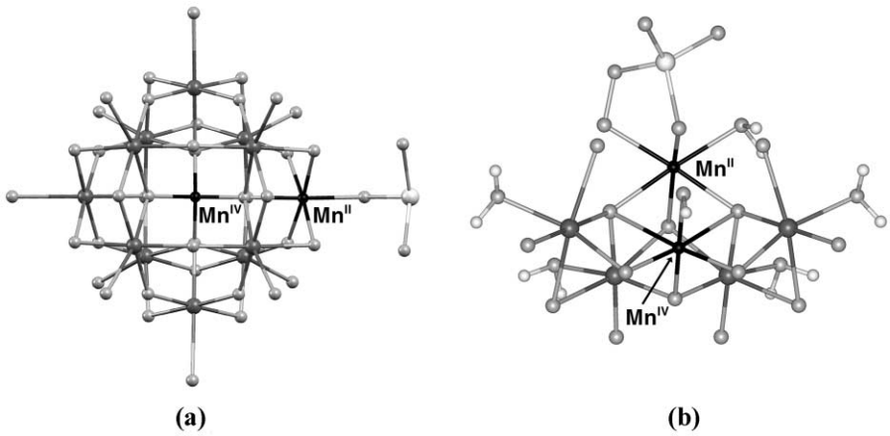

(a) (b)

Fig. 3 Representations of the heteropolyoxomolybdate units of the suggested transition states in the oxidations of Mn(II) by (a) BrO_3^- and (b) SO_5^{2-} in the presence of added molybdate.

(7)–(9) are fast compared to k_4, the actual oxidation and rate-determining step.

$$+d[MnMo_9O_{32}^{6-}]/dt = k_4[Mn^{IV}Mn^{II}(H_2O)Mo_{11}O_{39}^{6-}][BrO_3^-] \quad (16)$$

$$+d[MnMo_9O_{32}^{6-}]/dt = \frac{k_1k_2k_3k_4}{k_{-1}k_{-2}k_{-3}}[Mn^{2+}][Mn^{IV}Mo_9O_{32}^{6-}][HMoO_4^-]^2[BrO_3^-] \quad (17)$$

$$+d[MnMo_9O_{32}^{6-}]/dt = k_{AC(I)}[Mn^{2+}][Mn^{IV}Mo_9O_{32}^{6-}][HMoO_4^-]^2[BrO_3^-] \quad (18)$$

The transition state. Examination of the components of the rate-determining step gives, after arranging into a likely heteropolyoxomolybdate framework, a transition state that can be represented by $[Mn^{IV}Mn^{II}(H_2O)Mo_{11}O_{39}(BrO_3) \pm n(H_2O)]^{6-}$.[25] The structure of the "heteropolyoxomolybdate" moiety of the transition state (*i.e.* neglecting the oxidant) is a Mn(II)-substituted lacunary polyoxomolybdate with a Mn(IV) at the centre of the polyoxomolybdate framework, and is based on the Keggin structure. The heteropolyoxomolybdate structure is shown in Fig. 3(a), with the sixth coordination site around the Mn(II) filled by an oxygen of the BrO_3^- oxidant, following loss of the water molecule. Such a structure is feasible, as the tetrahedral crystal radius of Mn(IV) is identical to that of Ge(IV) (0.53 Å),[13] and Ge(IV) is commonly found at the centre of both intact (*e.g.* α-$[GeMo_{12}O_{40}]^{4-}$) and lacunary heteropolyoxometalates based on the Keggin structure.[26] The peripheral Mn(II) may readily lose a radially coordinated water molecule, as indicated by the above representation of the transition state, and be replaced by the oxidant. Indeed, water exchange of the related $[Mn(OH_2)_6]^{2+}$ is extremely rapid, with an exchange rate of 2.1×10^7 s^{-1} at 25 °C,[27] which correlates well with the zero crystal field stabilization energy for a high-spin d^5 electron configuration. Thus the BrO_3^- could coordinate through one of its oxygen atoms to the peripheral Mn(II) prior to electron transfer. Only monodentate coordination is possible, because of the constraints of the polyoxomolybdate framework. In order to investigate the likelihood of the Mn(II)-substituted lacunary heteropolyoxomolybdate as the transition state, extended-Hückel molecular orbital (EHMO) calculations were performed on the components of eqn. (19).

$$[Mn(OH_2)_6]^{2+} + [MnMo_9O_{32}]^{6-} + 2HMoO_4^- \longrightarrow [Mn^{IV}Mn^{II}Mo_{11}O_{39}]^{6-} + 7H_2O \quad (19)$$

For this equation, the change in total stabilization energy $\Delta E_T = E_T([Mn^{IV}Mn^{II}Mo_{11}O_{39}]^{6-}) + 7E_T(H_2O) - E_T([Mn(OH_2)_6]^{2+}) - E_T([MnMo_9O_{32}]^{6-}) - 2E_T(HMoO_4^-)$, where E_T for a particular species is the sum of the one-electron energies as calculated using the EHMO approach, is equal to $(-6215.24) + 7(-162.43) - (-1041.13) - (-5050.09) - 2(-628.96) = -3.11$ eV. It should be noted that no solvent considerations have been included in these calculations. In view of the approximations inherent in the EHMO method, the actual value of ΔE_T is not important, except to indicate that the products are energetically very similar to those of the reactants, given the individual values of E_T for the species involved. Moreover, if the β- (or even a γ-) form of the Keggin structure had been used for the $[Mn^{IV}Mn^{II}Mo_{11}O_{39}]^{6-}$ ion, the energy difference would have been even less, or indeed actually positive, as this isomeric form has been shown to be less energetically stable than the α-form (several eV using a similar calculational methodology).[28]

B. Oxidation of Mn(II) by HSO_5^- in the presence MoO_4^{2-}

The kinetics of oxidation of Mn(II) by HSO_5^- in the presence of molybdate under slightly acidic conditions at 30 °C also exhibited an "S-shaped" curve typical of an autocatalytic reaction, as found in the case of BrO_3^-. Previously, this system had been investigated at 40 °C, and the autocatalytic nature had been missed because of the compressed absorbance–time traces observed, so that the "induction" periods were overlooked. In that study, the kinetics were interpreted in terms of a first order system.[2] However, following the observation of the autocatalytic nature of the Mn(II)/molybdate system using HOCl[1] and BrO_3^- (the present study), the use of HSO_5^- as oxidant was re-investigated, but at lower temperatures, and its true autocatalytic nature revealed.

Oxidation of Mn(II) by HSO_5^- in the presence of molybdate over the pH range 4.4–5.5 occurred over a period of 5–30 minutes at room temperature for oxidant concentrations of 0.030–0.065 M. Again, the pH range is narrow because of the range of stability of the product species. Moreover, the reaction was incomplete below pH 4.4, based on the known molar absorptivity of $[MnMo_9O_{32}]^{6-}$, while complete conversion occurred above this value, up to a pH value of 5.5. All oxidation kinetics were subsequently recorded at 30 °C, with the exception of the temperature dependence study. Examination of a range of $[HSO_5^-]/[Mn^{2+}]$ values, with $[Mn^{2+}] = 0.0025$ M, $[MoO_4^{2-}] = 0.0625$ M and pH = 5.10 at 30.0 °C, indicated that the stoichiometry was 1.0 mole of HSO_5^- per mole of Mn^{2+}. The overall reaction can therefore be written as in eqn. (20).

$$Mn^{2+} + 9MoO_4^{2-} + 9H^+ + HSO_5^- \longrightarrow [MnMo_9O_{32}]^{6-} + 5H_2O + SO_4^{2-} \quad (20)$$

The kinetic data were analysed as described above in terms of a second order autocatalytic reaction. The rate constants and

Table 5 Observed rate constants for oxidation of Mn(II) by HSO_5^- in the presence of MoO_4^{2-}: oxidant dependence ($[Mn^{2+}]$ = 0.0025 M, $[MoO_4^{2-}]_T$ = 0.0625 M, pH = 5.29 ± 0.01, I = 1.00 M, 30.0 °C)

$[HSO_5^-]$/M	$k_{ac(2)}$/dm^3 mol^{-1} s^{-1}	$10^4[MnMo_9O_{32}^{6-}]_i$/M
0.030	8.0(4)	2.31
0.035	10.1(5)	1.96
0.045	13.7(5)	2.03
0.055	16.6(7)	1.96
0.065	20.9(9)	1.96

$[MnMo_9O_{32}^{6-}]_i$ data obtained under various conditions are given in Tables 5–8.

Dependences on HSO_5^-, H^+ and MoO_4^{2-}. The autocatalytic rate constant $k_{ac(2)}$ {eqn. (2), with $k_{ac(2)}$ replacing $k_{ac(1)}$ and subsuming dependences on $[HSO_5^-]$, $[H^+]$ and $[MoO_4^{2-}]$} showed a slight deviation from first order behaviour at pH 5.29 in the oxidant dependence. Thus a plot of log $k_{ac(2)}$ against log $[HSO_5^-]$ gave a linear relationship of slope 1.21(5) (R^2 = 0.9948), leading to rate expression (21).

$$+d[MnMo_9O_{32}^{6-}]/dt = k'_{ac(2)}[Mn^{2+}][MnMo_9O_{32}^{6-}][HSO_5^-]^{1.21} \quad (21)$$

The deviation from first order behaviour is well outside the limits of error in the data even considering the error in $k'_{ac(2)}$. A similar deviation from first order dependence was observed previously in the original study at pH 4.54,[2] and was also observed in the oxidation of Mn(II) by HOCl in the presence of molybdate at pH 4.49, although first order behaviour was observed under slightly less acidic conditions at pH 5.36.[1] Further treatment of the $[HSO_5^-]$ dependence is presented below.

The dependences of $k_{ac(2)}$ on both $[H^+]$ and $[MoO_4^{2-}]$ were obtained in a similar manner to those described above for the Mn(II)/molybdate/BrO_3^- system. The data are given in Tables 6 and 7, respectively. As found for oxidation by BrO_3^-, there is a complex non-linear dependence on pH, Fig. 4, and a non-linear dependence on total molybdate in solution, Fig. 5(a). For the molybdate dependence study, the range of concentrations studied was rather narrow (0.125–0.250 M), since below a $[MoO_4^{2-}]_T$ of 0.125 M the reaction did not go to completion. Although the pH dependence study was examined at a $[MoO_4^{2-}]_T$ of 0.0625 M the ionic strength was lower, and resulted in complete reaction. It thus appears that at higher ionic strengths and lower total molybdate concentrations the oxidation reaction is incomplete. Again, assuming that the differences in molybdate speciation under the experimental conditions of this study and those employed in the estimation

Table 8 Observed rate constants for oxidation of Mn(II) by HSO_5^- in the presence of MoO_4^{2-}: temperature dependence ($[Mn^{2+}]$ = 0.0025 M, $[HSO_5^-]$ = 0.060 M, $[MoO_4^{2-}]_T$ = 0.0625 M, pH = 5.25, I = 1.00 M)

Temperature/°C	$k_{ac(2)}$/dm^3 mol^{-1} s^{-1}	$10^4[MnMo_9O_{32}^{6-}]_i$/M
15.0	6.6(3)	2.36
20.0	8.2(4)	1.60
25.1	10.2(5)	1.88
29.8	12.0(5)	1.95
34.7	13.9(6)	1.87

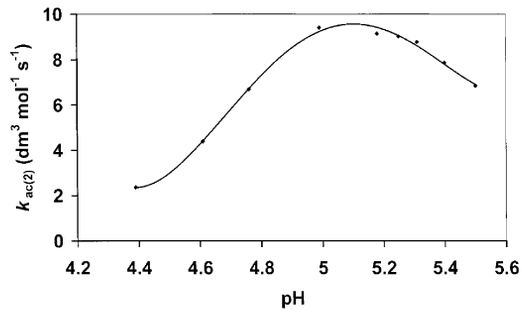

Fig. 4 Dependence of $k_{ac(2)}$ on pH. $[Mn^{2+}]$ = 0.0025 M, $[HSO_5^-]$ = 0.030 M, $[MoO_4^{2-}]_T$ = 0.0625 M, I = 1.00 M, 30.0 °C.

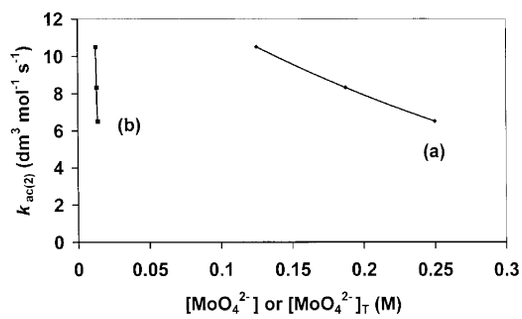

Fig. 5 Dependence of $k_{ac(2)}$ on (a) total added molybdate, $[MoO_4^{2-}]_T$ and (b) actual $[MoO_4^{2-}]$ in solution. $[Mn^{2+}]$ = 0.0025 M, $[HSO_5^-]$ = 0.030 M, pH = 5.20, I = 1.50 M, 30.0 °C.

Table 6 Observed rate constants for oxidation of Mn(II) by HSO_5^- in the presence of MoO_4^{2-}: pH dependence ($[Mn^{2+}]$ = 0.0025 M, $[HSO_5^-]$ = 0.030 M, $[MoO_4^{2-}]_T$ = 0.0625 M, I = 1.00 M, 30.0 °C)

pH	$10^2[MoO_4^{2-}]_{calc}$/M	$k_{ac(2)}$/dm^3 mol^{-1} s^{-1}	$10^4[MnMo_9O_{32}^{6-}]_i$/M
4.39	0.133	2.4(1)	3.12
4.61	0.237	4.4(2)	3.30
4.76	0.351	6.7(3)	2.36
4.99	0.639	9.4(4)	1.87
5.18	1.04	9.1(4)	1.29
5.25	1.25	9.0(4)	1.72
5.31	1.45	8.8(4)	1.85
5.40	1.82	7.9(4)	2.04
5.50	2.32	6.9(3)	2.68

Table 7 Observed rate constants for oxidation of Mn(II) by HSO_5^- in the presence of MoO_4^{2-}: molybdate dependence ($[Mn^{2+}]$ = 0.0025 M, $[HSO_5^-]$ = 0.030 M, pH = 5.20 ± 0.01, I = 1.50 M, 30.0 °C)

Total $[MoO_4^{2-}]$/M	$10^2[MoO_4^{2-}]_{calc}$/M	$k_{ac(2)}$/dm^3 mol^{-1} s^{-1}	$10^4[MnMo_9O_{32}^{6-}]_i$/M
0.125	1.26	10.5(5)	1.62
0.1875	1.31	8.3(4)	1.60
0.250	1.40	6.5(3)	2.12

of the formation constants are not great, then the actual MoO_4^{2-} concentrations in solution, *i.e.* $[MoO_4^{2-}]_{calc}$, for various amounts of total added molybdate, at constant pH, may be used to investigate the $[MoO_4^{2-}]$ dependence. The variation of $k_{ac(2)}$ with $[MoO_4^{2-}]_{calc}$ is given in Fig. 5(b). A plot of log $k_{ac(2)}$ against log $[MoO_4^{2-}]_{calc}$ produced an inverse relationship with a slope of −4.92(60) (R^2 = 0.9752), which indicates an inverse fifth-order dependence on $[MoO_4^{2-}]_{calc}$, although the error is somewhat large because of the restricted range of total molybdate concentrations available. This results in the new rate expression (22).

$$+d[MnMo_9O_{32}^{6-}]/dt = k''_{ac(2)}[Mn^{2+}][MnMo_9O_{32}^{6-}][MoO_4^{2-}]^{-5}[HSO_5^-]^{1.21} \quad (22)$$

Similarly, a plot of log $\{k_{ac(2)}/[MoO_4^{2-}]^{-5}\}$, using the appropriate $[MoO_4^{2-}]_{calc}$ values, against log $[H^+]$ yields a linear relationship of slope −6.01(14) (R^2 = 0.9962), indicating an inverse sixth-order dependence on $[H^+]$. The rate expression can be further expanded to include this dependence, as in eqn. (23).

$$+d[MnMo_9O_{32}^{6-}]/dt = k'''_{ac(2)}[Mn^{2+}][MnMo_9O_{32}^{6-}][MoO_4^{2-}]^{-5}[H^+]^{-6}[HSO_5^-]^{1.21} \quad (23)$$

Now, for the range of acidity employed in these studies the primary molybdate species is $HMoO_4^-$ rather than MoO_4^{2-}, as noted above. Again, using the protonation equilibrium $H^+ + MoO_4^{2-} \leftrightarrow HMoO_4^-$, rate expression (23) can be rewritten as eqn. (24).

$$+d[MnMo_9O_{32}^{6-}]/dt = k''''_{ac(2)}[Mn^{2+}][MnMo_9O_{32}^{6-}][HMoO_4^-]^{-5}[H^+]^{-1}[HSO_5^-]^{1.21} \quad (24)$$

With this rate expression in hand, the non-integral exponent of the oxidant term can be addressed, and suggests an alternative form of the above rate expression involving two parallel pathways, one dependent on HSO_5^- and the other on SO_5^{2-}. For the reaction $HSO_5^- \leftrightarrow SO_5^{2-} + H^+$, the $K_a = 4.0(9) \times 10^{-10}$.[29] Combination of this relationship with eqn. (24) results in rate expression (25), where $k_{AC(2a)} = 4.6(4) \times 10^{-11}$ dm^{-9} mol^3 s^{-1} and $k_{AC(2b)} = 2.6(4) \times 10^{-15}$ dm^{-9} mol^3 s^{-1}.

$$+d[MnMo_9O_{32}^{6-}]/dt = k_{AC(2a)}[Mn^{2+}][MnMo_9O_{32}^{6-}][HMoO_4^-]^{-5}[SO_5^{2-}] + k_{AC(2b)}[Mn^{2+}][MnMo_9O_{32}^{6-}][HMoO_4^-]^{-5}[HSO_5^-] \quad (25)$$

It should be noted that previously, SO_5^{2-} has been shown to be the active oxidant under acidic conditions in the slow oxidation of $[Co^{II}W_{12}O_{40}]^{6-}$ to $[Co^{III}W_{12}O_{40}]^{5-}$.[5] The emergence of the second pathway in the rate law above suggests that HSO_5^- acts as the preferred oxidant in acidic medium, while the deprotonated species SO_5^{2-} becomes the more favoured oxidant under less acidic conditions and also kinetically slow oxidation conditions.

Temperature dependence. The temperature dependence was studied from 15.0–34.7 °C at pH 5.25, and the data are given in Table 8. An Arrhenius plot of ln $k_{ac(2)}$ against $1/T$ produced a linear relationship (R^2 = 0.9962) and an Arrhenius activation energy, E_a, of 28 kJ mol^{-1}. The linear nature of the plot suggests that there is negligible change in speciation in the actual $[MoO_4^{2-}]$ in solution resulting from any change in molybdate polymerization over the temperature range examined, which is close to the actual temperatures used for the determination of the stability constants. The data in Table 8 may also be used to estimate the enthalpies and entropies of activation for both oxidative pathways, using autocatalytic rate constants from which the pseudo concentration dependences on $[MoO_4^-]$, $[H^+]$ and [oxidant] have been removed. The data give $\Delta H^{\ddagger} \approx 26$ kJ mol^{-1} for both pathways and $\Delta S^{\ddagger} \approx -900$ and −800 J K^{-1} mol^{-1} for the major (SO_5^{2-} oxidation) and minor (HSO_5^- oxidation) pathways, respectively. As solvation effects dominate in reactions between ionic species, the large negative activation entropies for both pathways indicate significant solvent rearrangement during formation of the transition state, likely involving a large increase in solvation, particularly of the dissociated $HMoO_4^-$ ions, in forming the transition states of the two pathways.

Mechanistic considerations. The rate expression established above suggests that, prior to oxidation, five monomeric protonated molybdate units are lost from an initial Mn(II)–Mn(IV)-polyoxomolybdate anion (*i.e.* $[Mn^{II}Mn^{IV}Mo_9O_{32}]^{4-}$). This "unwrapping" allows the oxidant (SO_5^{2-} or HSO_5^-) to enter the primary coordination sphere of the Mn(II) and effect a two-electron oxidation of Mn(II) to Mn(IV), probably as two sequential one-electron steps. The loss of the five $HMoO_4^-$ units likely exposes the Mn(II) so that it can be coordinated in a bidentate manner, a coordination mode that can also be inferred in the oxidation of Co(II) by HSO_5^- in the presence of molybdate to give $[H_4Co_2Mo_{10}O_{38}]^{6-}$.[4] If either oxidant ($SO_5^{2-}$ or HSO_5^-) were to favour monodentate coordination, then the rate law would likely have been similar to that with BrO_3^- as oxidant.

The mechanism of oxidation can be expressed by equilibria (26)–(33), in which the rate-determining steps are (32a) and (32b) for the major and minor pathways, respectively.

$$Mn^{II} + [Mn^{IV}Mo_9O_{32}]^{6-} \underset{k_{-1}}{\overset{k_1}{\rightleftharpoons}} [Mn^{II}Mn^{IV}Mo_9O_{32}]^{4-} \quad (26)$$

$$[Mn^{II}Mn^{IV}Mo_9O_{32}]^{4-} + H_2O \underset{k_{-2}}{\overset{k_2}{\rightleftharpoons}} [Mn^{II}Mn^{IV}Mo_8O_{29}H]^{3-} + HMoO_4^- \quad (27)$$

$$[Mn^{II}Mn^{IV}Mo_8O_{29}H]^{3-} \underset{k_{-3}}{\overset{k_3}{\rightleftharpoons}} [Mn^{II}Mn^{IV}Mo_7O_{25}]^{2-} + HMoO_4^- \quad (28)$$

$$[Mn^{II}Mn^{IV}Mo_7O_{25}]^{2-} + H_2O \underset{k_{-4}}{\overset{k_4}{\rightleftharpoons}} [Mn^{II}Mn^{IV}Mo_6O_{22}H]^- + HMoO_4^- \quad (29)$$

$$[Mn^{II}Mn^{IV}Mo_6O_{22}H]^- \underset{k_{-5}}{\overset{k_5}{\rightleftharpoons}} [Mn^{II}Mn^{IV}Mo_5O_{18}]^0 + HMoO_4^- \quad (30)$$

$$[Mn^{II}Mn^{IV}Mo_5O_{18}]^0 + H_2O \underset{k_{-6}}{\overset{k_6}{\rightleftharpoons}} [Mn^{II}Mn^{IV}Mo_4O_{15}H]^+ + HMoO_4^- \quad (31)$$

$$[Mn^{II}Mn^{IV}Mo_4O_{15}H]^+ + SO_5^{2-} \xrightarrow{k_7} [Mn^{IV}Mn^{IV}Mo_4O_{15}HSO_5]^- \quad (32a)$$

$$[Mn^{II}Mn^{IV}Mo_4O_{15}H]^+ + HSO_5^- \xrightarrow{k_8} [Mn^{IV}Mn^{IV}Mo_4O_{15}H_2SO_5]^0 \quad (32b)$$

$$[Mn^{IV}Mn^{IV}Mo_4O_{15}HSO_5]^- + 14MoO_4^{2-} + 15H^+ \longrightarrow 2[MnMo_9O_{32}]^{6-} + 8H_2O + SO_4^{2-} \quad (33a)$$

$$[Mn^{IV}Mn^{IV}Mo_4O_{15}H_2SO_5]^0 + 14MoO_4^{2-} + 14H^+ \longrightarrow 2[MnMo_9O_{32}]^{6-} + 8H_2O + SO_4^{2-} \quad (33b)$$

It should be noted that the above equations have been written without the express involvement of solvent, except where water molecules are required for correct stoichiometry.

Water molecules are assumed to be involved in rapid loss/addition to Mn(II) and Mn(IV), presumably maintaining six coordination around these ions, and also in solvation of the $HMoO_4^-$ ions. The rate determining steps, (32a) and (32b), are followed by fast reactions (33a) and (33b), which involve, in either case, the breakdown of the double Mn(IV)-containing species and the assembly of the polyoxomolybdate framework around each Mn(IV) centre. Combination of steps (26)–(31) with either (32a) and (33a), or with (32b) and (33b), yields the stoichiometry given above in eqn. (20).

Now, from the fast equilibria (26)–(31), expression (34) can be derived.

$$[Mn^{II}Mn^{IV}Mo_4O_{15}H^+] = \frac{k_1k_2k_3k_4k_5k_6}{k_{-1}k_{-2}k_{-3}k_{-4}k_{-5}k_{-6}}[Mn^{2+}][Mn^{IV}Mo_9O_{32}{}^{6-}][HMoO_4^-]^{-5} \quad (34)$$

Also, from eqns. (32a) and (32b) the two-term kinetic equation for the rate-determining step is given by (35).

$$+d[MnMo_9O_{32}{}^{6-}]/dt = k_7[Mn^{II}Mn^{IV}Mo_4O_{15}H^+][SO_5^{2-}] + k_8[Mn^{II}Mn^{IV}Mo_4O_{15}H^+][HSO_5^-] \quad (35)$$

Combining eqns. (34) and (35) gives eqn. (36) for the rate-determining step, which may then be written as (37), where $k_{(2a)}' = k_1k_2k_3k_4k_5k_6k_7/k_{-1}k_{-2}k_{-3}k_{-4}k_{-5}k_{-6}$ and $k_{(2b)}' = k_1k_2k_3k_4k_5k_6k_8/k_{-1}k_{-2}k_{-3}k_{-4}k_{-5}k_{-6}$. This is equivalent to eqn. (25), with $k_{(2a)}' = k_{AC(2a)}$ and $k_{(2b)}' = k_{AC(2b)}$, assuming that the pre-equilibria (26)–(31) are faster than the rate-determining steps (32a) and (32b).

$$+d[MnMo_9O_{32}{}^{6-}]/dt = \frac{k_1k_2k_3k_4k_5k_6k_7}{k_{-1}k_{-2}k_{-3}k_{-4}k_{-5}k_{-6}}[Mn^{2+}][MnMo_9O_{32}{}^{6-}][HMoO_4^-]^{-5}[SO_5^{2-}] + \frac{k_1k_2k_3k_4k_5k_6k_8}{k_{-1}k_{-2}k_{-3}k_{-4}k_{-5}k_{-6}}[Mn^{2+}][MnMo_9O_{32}{}^{6-}][HMoO_4^-]^{-5}[HSO_5^-] \quad (36)$$

$$+d[MnMo_9O_{32}{}^{6-}]/dt = k_{(2a)}'[Mn^{2+}][MnMo_9O_{32}{}^{6-}][HMoO_4^-]^{-5}[SO_5^{2-}] + k_{(2b)}'[Mn^{2+}][MnMo_9O_{32}{}^{6-}][HMoO_4^-]^{-5}[HSO_5^-] \quad (37)$$

The rate law and mechanism are consistent with a series of fast equilibria involving the original formation of a Mn^{II}–Mn^{IV}-polyoxomolybdate anion (required to create the observed autocatalysis) followed by sequential loss of $HMoO_4^-$ (or H^+ and MoO_4^{2-}) from this species. The substrate actually oxidised can reasonably be assumed to be a solvated $[Mn^{II}Mn^{IV}Mo_4O_{15}H]^+$ ion. Exchange of water molecules is presumably very fast, allowing facile coordination of SO_5^{2-} in the major pathway and HSO_5^- in the minor pathway, subsequently leading to a two-electron oxidation of Mn(II) to Mn(IV). Electron transfer is facilitated by coordination, and is effectively intramolecular. Notably, both oxidant species coordinate to a species with a positive charge, which is electrostatically favoured, and which also favours SO_5^{2-} over HSO_5^-, which is consistent with the former oxidant participating in the major oxidative pathway. Both oxidation steps must be slower than the reversible loss of $HMoO_4^-$ from the labile precursor, and hence oxidation is the rate-determining step(s). Following oxidation, fast ligand reorganization/breakdown is assumed to occur which most likely involves a rearrangement of the primary coordination sphere of the newly oxidised Mn(IV) and/or breakdown of the reduced "SO_5^{4-}" or "HSO_5^{2-}" ligand to SO_4^{2-} and an O^{2-} or OH^- ion, which then ends up protonated as H_2O. This step was not kinetically observed, which indicates a fast change in the nature of the immediate oxidation product. At some stage this must involve separation of the two Mn(IV) centres, while any ligand replacement would involve exchange of the weakly coordinated SO_4^{2-} by MoO_4^{2-}. The resulting separated Mn^{IV} centres have only partially built polyoxomolybdate environments and so would undergo fast $HMoO_4^-$ (or MoO_4^{2-}) addition to yield the observed product species, $[MnMo_9O_{32}]^{6-}$. Interestingly, the mechanism of oxidation of Co(II) by HSO_5^- in the presence of molybdate is similar,[4] in that it also involves a series of fast equilibria involving loss of three $HMoO_4^-$ ions and one H^+ from $[H_6Co^{II}Mo_6O_{24}]^{4-}$ to give solvated "$[H_2Co^{II}Mo_3O_{12}]^{2-}$", which is subsequently oxidised by the coordinated oxidant. Although the inverse $[H^+]$ dependence in the rate law obtained in that study could be a reflection of the involvement of SO_5^{2-} rather than HSO_5^- as oxidant, it is considered that HSO_5^- is the oxidant as that reaction is kinetically quite fast, unlike in the present case. It is suggested that the emergence of a pathway involving SO_5^{2-} occurs only under kinetically slow reaction conditions.

The transition state. Examination of the components of the rate-determining step gives a transition state that can be represented by $[Mn^{II}Mn^{IV}Mo_4O_{15}H(HSO_5 \text{ or } SO_5) \pm n(H_2O)]^{(0 \text{ or } 1-)}$.[25] The most compact polyoxometalate structure for six metal atoms involving only edge bridging is that of $[Mo_6O_{19}]^{2-}$. Thus in the above transition state there is already a deficit of oxygen atoms and several water molecules must be included in the structure (*i.e.* $n > 0$ in the above formulation). (Although face sharing of neighbouring polyoxometalate polyhedra could be considered, this would lead to three oxo bridges between the transition metal atoms and much less likelihood of labile monomeric molybdate or manganese units.) However, in the $[Mo_6O_{19}]^{2-}$ structure each metal atom has only one terminal oxygen atom, and the evidence presented above suggests that bidentate coordination of the oxidant (SO_5^{2-} or HSO_5^-) is necessary. A more open structure would be required, and a plausible transition state can be built from a fragment of a Mn(IV)-centred Anderson structure, with a capping hydrated Mn(II) ion, as shown in Fig. 3(b). It should be noted that Mn(IV) at the core of an Anderson structure is known in $Na_8[Mn^{IV}W_6O_{24}]\cdot 18H_2O$.[30] The proposed structure involves the Mn(IV) bordered by four molybdate units that are edge-bridged to each other and to the "central" Mn(IV). The latter thus has five oxo bridging ligands. As an unprotected Mn(IV) is capable of oxidizing water, it can easily be protected if the sixth coordination site is assumed to be a hydroxo ligand, involving the one H atom in the transition state (neglecting the water molecules). The Mn(II) does not take up another position that would generate the planar Anderson structure as no room would be left for the HSO_5^-/SO_5^{2-} oxidant to easily coordinate to the Mn(II). Rather, it can be placed on top of the central Mn(IV), thereby sharing three oxo ligands. Assuming six coordination of the Mn(II) in this transition state, as is likely, the other three coordination sites can be occupied by the oxidant in a bidentate manner and the other by a water molecule. In Fig. 3(b) the three sites have been shown occupied by a water molecule and SO_5^{2-} oxidant anion, the latter the major oxidant, although it could easily be replaced by a HSO_5^- oxidant anion. The four octahedrally coordinated Mo(VI) ions have either one or two terminal oxo ligands and all have one water molecule, with the latter poised to accept an oxo ligand of another monomeric molybdate unit and begin the generation of the complete polyoxomolybdate frameworks around the two (separated) Mn(IV) centres following oxidation of the Mn(II) to Mn(IV).

BrO_3^- *versus* HSO_5^-/SO_5^{2-} oxidation. A comparison between the two systems indicates that the polyoxomolybdate framework behaves differently in the cases detailed in the present work. This is likely dictated by the mode of electron transfer that is favoured by the two oxidants, BrO_3^- and HSO_5^-/SO_5^{2-}. In the former case, coordination through a single oxygen atom would seem to be preferred given the single coordination site available in the lacunary structure, although

electron transfer across the polyoxomolybdate framework is also possible, as occurs in the oxidation of the α-Keggin structure of $[Co^{II}W_{12}O_{40}]^{6-}$ to $[Co^{III}W_{12}O_{40}]^{5-}$ under highly acidic conditions using a variety of oxidants.[5,23,31–33] This is, however, a result of the robustness of the polyoxotungstate framework under such highly acidic conditions. In the case of oxidation by both HSO_5^- and SO_5^{2-}, however, in order to account for the difference in the mechanism, it would appear that both of these oxidants require bidentate coodination to effect electron transfer. The "labile" polyoxomolybdate framework over the pH range investigated is able to accommodate these requirements because of the facile loss of $HMoO_4^-$ (or H^+ and MoO_4^{2-}). It should be stressed that the presence of molybdate, despite highlighting the difference in the two oxidants, plays an important role in both systems in that the final Mn(IV)-containing species in each case is the soluble $[MnMo_9O_{32}]^{6-}$ ion, rather than, say, MnO_2.

Finally, re-examination of the experimental rate law determined for the oxidation of Mn(II) by HOCl in the presence of added molybdate at pH 4.0–5.4 and 20 °C,[1] shows that it can be written as eqn. (38).

$$+d[MnMo_9O_{32}^{6-}]/dt = k_{AC(3)}[Mn^{2+}][Mn^{IV}Mo_9O_{32}^{6-}][HMoO_4^-]^2[OCl^-] \quad (38)$$

This is identical with rate eqn. (18), except that BrO_3^- has been replaced by OCl^- as the oxidant. Presumably, the latter is the actual oxidant rather than HOCl, as was postulated originally, which is feasible as the pK_a of HOCl is 7.53 at 25 °C.[34] Thus the form of the transition state is the same as proposed for BrO_3^- oxidation, with the OCl^- oxidant singly coordinated through its oxygen atom.

In conclusion, therefore, oxidation of Mn(II) by BrO_3^- and HSO_5^- in the presence of molybdate both follow an autocatalytic mechanism (as does oxidation by OCl^-), with the product species actively involved in formation of the transition states of the reactions. These can be interpreted in terms of the well-known Keggin and Anderson structures that are exhibited by polyoxometalates, with the latter generated by loss of monomeric $HMoO_4^-$ units. The differences in behaviour of the polyoxmolybdate framework (*i.e.* rearrangement to give a Keggin-type structure for BrO_3^- oxidation, and fragmentation to an Anderson-related structure for HSO_5^- oxidation) are related to the coordination of the oxidant (mono- and bi-dentate, respectively). This likely stems from the requirements of the electron transfer processes of the two oxidants. Finally, from a comparison of the three rate laws, the species $HMoO_4^-$ is now firmly established as the primary building block for polyoxomolybdate formation.

Acknowledgements

We would like to acknowledge receipt of an Australian Post-graduate Research Award (to A. L. N.). We would also like to thank Mr G. DeIuliis for help in the preparation of Fig. 3.

References

1 S. J. Angus-Dunne, J. A. Irwin, R. C. Burns, G. A. Lawrance and D. C. Craig, *J. Chem. Soc., Dalton Trans.*, 1993, 2717.
2 S. J. Dunne, R. C. Burns, T. W. Hambley and G. A. Lawrance, *Aust. J. Chem.*, 1992, **45**, 685.
3 S. J. Dunne, R. C. Burns and G. A. Lawrance, *Aust. J. Chem.*, 1992, **45**, 1943.
4 A. L. Nolan, R. C. Burns and G. A. Lawrance, *J. Chem. Soc., Dalton Trans.*, 1996, 2629.
5 A. L. Nolan, R. C. Burns and G. A. Lawrance, *J. Chem. Soc., Dalton Trans.*, 1998, 3041.
6 W. Stumm and J. J. Morgan, *Aquatic Chemistry*, Wiley-Interscience, NY, 1970.
7 Ya. D. Tiginyanu, A. P. Moravskii, V. F. Shuvalov and V. M. Bernikov, *Kinet. Katal. (Engl. Transl.)*, 1983, **24**, 5.
8 A. L. Nolan, S. J. Angus-Dunne, J. A. Irwin, R. C. Burns, G. A. Lawrance and D. C. Craig, in preparation.
9 D. K. Walanda, R. C. Burns, G. A. Lawrance and E. I. von Nagy-Felsobuki, *J. Chem. Soc., Dalton Trans.*, 1999, 311.
10 D. K. Walanda, R. C. Burns, G. A. Lawrance and E. I. von Nagy-Felsobuki, *J. Cluster Sci.*, 2000, **11**, 5.
11 C. Mealli and D. M. Proserpio, *J. Chem. Educ.*, 1990, **67**, 399.
12 R. Strandberg, *Acta Crystallogr., Sect. B*, 1977, **33**, 3090.
13 R. D. Shannon, *Acta Crystallogr., Sect. A*, 1976, **32**, 751.
14 F. A. Cotton, L. M. Daniels, C. A. Murillo and J. F. Quesada, *Inorg. Chem.*, 1993, **32**, 4861.
15 L. C. W. Baker and T. J. R. Weakley, *J. Inorg. Nucl. Chem.*, 1966, **28**, 447.
16 N. M. Emanuel' and D. G. Knorre, *Chemical Kinetics Homogeneous Reactions*, Wiley, NY, 1973, p.271.
17 T. Ozeki, H. Kihara and S. Hikime, *Anal. Chem.*, 1987, **59**, 945.
18 T. Ozeki, H. Kihara and S. Ikeda, *Anal. Chem.*, 1988, **60**, 2055.
19 K. H. Tytko, G. Baethe, E. R. Hirschfeld, K. Mehmke and D. Stellhorn, *Z. Anorg. Allg. Chem.*, 1983, **503**, 43.
20 J. P. Birk and S. G. Kozub, *Inorg. Chem.*, 1973, **12**, 2460.
21 J. P. Birk, *Inorg. Chem.*, 1978, **17**, 504.
22 J. P. Birk and S. G. Kozub, *Inorg. Chem.*, 1978, **17**, 1186.
23 G. A. Ayoko, J. F. Iyun and I. F. El-Idris, *Transition Met. Chem.*, 1991, **16**, 145.
24 J. P. Birk, *Inorg. Chem.*, 1973, **12**, 2468.
25 J. H. Espenson, *Chemical Kinetics and Reaction Mechanisms*, 2nd edn., McGraw-Hill, NY, 1995, ch.6, p.125.
26 M. T. Pope, *Heteropoly and Isopoly Oxometalates*, Springer, Berlin, 1983.
27 R. B. Jordan, *Reaction Mechanisms of Inorganic and Organometallic Systems*, Oxford University Press, NY, 1991, p. 69.
28 S.-H. Wang and S. A. Jansen, *Chem. Mater.*, 1994, **6**, 2130.
29 D. L. Ball and J. O. Edwards, *J. Am. Chem. Soc.*, 1956, **78**, 1125.
30 A. L. Nolan, R. C. Burns, G. A. Lawrance and D. C. Craig, *Acta Crystallogr., Sect. C*, 2000, **56**, 729.
31 G. A. Ayoko, J. F. Iyun and I. F. El-Idris, *Transition Met. Chem.*, 1992, **17**, 46.
32 G. A. Ayoko, J. F. Iyun and I. F. El-Idris, *Transition Met. Chem.*, 1992, **17**, 423.
33 G. A. Ayoko, J. F. Iyun and I. F. El-Idris, *Transition Met. Chem.*, 1994, **19**, 212.
34 *Critical Stability Constants*, R. M. Smith and A. E. Martell, eds., Plenum, NY, 1976, vol. 4.